Basic Research in Cardiology (2020) 115:59
https://doi.org/10.1007/s00395-020-00820-0

ORIGINAL CONTRIBUTION

Intracellular O-linked glycosylation directly regulates cardiomyocyte L-type Ca^{2+} channel activity and excitation–contraction coupling

Andrew R. Ednie[1] · **Eric S. Bennett**[1]

Received: 8 May 2020 / Accepted: 17 August 2020 / Published online: 10 September 2020

Abstract

Cardiomyocyte L-type Ca^{2+} channels (Ca_vs) are targets of signaling pathways that modulate channel activity in response to physiologic stimuli. Ca_v regulation is typically transient and beneficial but chronic stimulation can become pathologic; therefore, gaining a more complete understanding of Ca_v regulation is of critical importance. Intracellular O-linked glycosylation (O-GlcNAcylation), which is the result of two enzymes that dynamically add and remove single N-acetylglucosamines to and from intracellular serine/threonine residues (OGT and OGA respectively), has proven to be an increasingly important post-translational modification that contributes to the regulation of many physiologic processes. However, there is currently no known role for O-GlcNAcylation in the direct regulation of Ca_v activity nor is its contribution to cardiac electrical signaling and EC coupling well understood. Here we aimed to delineate the role of O-GlcNAcylation in regulating cardiomyocyte L-type Ca_v activity and its subsequent effect on EC coupling by utilizing a mouse strain possessing an inducible cardiomyocyte-specific OGT-null-transgene. Ablation of the OGT-gene in adult cardiomyocytes (OGTKO) reduced OGT expression and O-GlcNAcylation by > 90%. Voltage clamp recordings indicated an ~ 40% reduction in OGTKO Ca_v current (I_{Ca}), but with increased efficacy of adrenergic stimulation, and Ca_v steady-state gating and window current were significantly depolarized. Consistently, OGTKO cardiomyocyte intracellular Ca^{2+} release and contractility were diminished and demonstrated greater beat-to-beat variability. Additionally, we show that the Ca_v $\alpha 1$ and $\beta 2$ subunits are O-GlcNAcylated while $\alpha 2\delta 1$ is not. Echocardiographic analyses indicated that the reductions in OGTKO cardiomyocyte Ca^{2+} handling and contractility were conserved at the whole-heart level as evidenced by significantly reduced left-ventricular contractility in the absence of hypertrophy. The data indicate, for the first time, that O-GlcNAc signaling is a critical and direct regulator of cardiomyocyte I_{Ca} achieved through altered Ca_v expression, gating, and response to adrenergic stimulation; these mechanisms have significant implications for understanding how EC coupling is regulated in health and disease.

Keywords Cardiomyocyte · Voltage-gated Ca^{2+} channel · EC coupling · O-GlcNAc · Isoproterenol · Ion channel gating

Introduction

The transient addition of a single N-acetylglucosamine (GlcNAc) to intracellular serine/threonine residues (O-GlcNAcylation) is a ubiquitous post-translational modification that contributes to the regulation of a variety of proteins and physiologic processes [29]. O-GlcNAcylation occurs through activity of two enzymes: O-linked β-N-acetylglucosamine transferase (OGT) and O-linked β-N-acetyl glucosaminase (OGA), which, under normal physiologic conditions, dynamically add and remove GlcNAc residues respectively [29]. Production of the OGT substrate, UDP-GlcNAc, requires processing of metabolites such as glucose, acetyl-coA and glutamine through the hexosamine biosynthesis pathway [50] and was shown to be increased in diabetic conditions [19, 50]; thus, OGT is also often referred to as a nutrient sensor. In addition to those activities common to all cell types including transcription, translation and cellular metabolism [29], O-GlcNAcylation plays an important role in a variety of physiologic processes specific

Electronic supplementary material The online version of this article (https://doi.org/10.1007/s00395-020-00820-0) contains supplementary material, which is available to authorized users.

✉ Andrew R. Ednie
andrew.ednie@wright.edu

[1] Department of Neuroscience, Cell Biology and Physiology, Boonshoft School of Medicine and College of Science and Mathematics, Wright State University, 143 Biological Sciences II, 3640 Colonel Glenn Hwy, Dayton, OH 45435, USA

to cardiomyocyte function including ischemia–reperfusion injury and hypertrophic signaling [4, 20, 39]; however, its role in excitation–contraction (EC) coupling has only recently begun to emerge, and primarily studied only in the context of diabetes/hyperglycemia [9, 13, 19, 31, 52, 53, 55, 68].

L-type voltage-gated Ca^{2+} channels (Ca_vs), which are putatively formed by the assembly of α1 ($Ca_v1.2$), α2δ1 and β2 subunits, trigger cardiomyocyte Ca^{2+}-activated Ca^{2+}-release and can be directly targeted by signaling pathways that allow the heart to respond to physiologic cues [5, 38]. This modulation of Ca_v activity is typically transient and beneficial; however, chronic disease states such as hypertrophic cardiomyopathy and diabetes often appropriate these adaptive signaling pathways such that they become pathologic [8, 22, 38, 59]. Several studies demonstrated that cardiac Ca_v activity is depressed in chronic diabetic models [45, 48, 63]; although, the mechanisms are not well understood. Additionally, utilizing a proteomics approach, it was suggested that several neuronal Ca_v subunit isoforms bear the O-GlcNAc modification [62]. Despite these findings, a potential role for the regulation of cardiomyocyte Ca_vs by O-GlcNAcylation is currently unknown.

Here we sought to determine the inherent functional impact of O-GlcNAcylation on cardiac L-type Ca_v activity by utilizing an inducible cardiomyocyte specific OGT-gene deficient mouse strain (OGTKO). Following induction, OGTKO cardiomyocytes demonstrated significant reductions in Ca_v current (I_{Ca}), with concomitant reductions in Ca_v $\alpha 1$ and $\beta 2$ expression, but with increased efficacy of adrenergic stimulation. OGTKO cardiomyocytes also demonstrated depolarizing shifts in Ca_v voltage-dependent steady-state gating. Consistently, intracellular Ca^{2+} release and contractility were diminished in OGTKO cardiomyocytes with concurrent reductions in left-ventricular (LV) contractility. We also observed that cardiac Ca_v $\alpha 1$ and $\beta 2$ subunits bear the O-GlcNAc modification, while the $\alpha 2\delta 1$ subunit does not. Thus, results from this study indicate, for the first time, that O-GlcNAc signaling, under basal and non-diseased related conditions, is a crucial and direct regulator of cardiomyocyte L-type Ca_v activity and therefore EC coupling.

Methods

Ethical approval

Animals were handled in accordance with the NIH Guide for the Care and Use of Laboratory Animals. All protocols involving animals were approved by the Wright State University Institutional Animal Care and Use Committee. Mice were euthanized, under deep anesthesia (5% isoflurane), by thoracotomy and excision of the heart to obtain samples for the biochemical and functional studies.

Generation of the OGTKO and animal use

12–16 week-old male mice were used in all experiments. To create the OGTKO strain, female mice homozygous for a transgene possessing loxP sites flanking the exon encoding amino acids 206–232 of the X-linked OGT gene (004860; The Jackson Laboratory, Bar Harbor, ME, USA) were crossed with male mice possessing one copy of the α-MHC-MerCreMer transgene, which consists of a cardiac-specific α-myosin heavy chain promoter directing expression of a tamoxifen-inducible Cre recombinase (005657; The Jackson Laboratory). Cre expression and OGT gene deletion were accomplished by intraperitoneal injection of tamoxifen (75mgs/kg; T5658; MilliporeSigma, Burlington, MA, USA) dissolved in corn oil (C8267; MilliporeSigma) for four consecutive days. To control for potential spurious effects of tamoxifen injection and α-MHC-MerCreMer expression [6], all control mice were tamoxifen treated and α-MHC-MerCreMer positive but had a normal OGT gene. Animals were used 18–30 days post induction (dpi).

Cardiomyocyte isolation

Cardiomyocytes from the LV wall were isolated using 1 mg/ml collagenase type II (CLS2; Worthington Biochemical, Lakewood, NJ, USA) and 0.65 u/ml protease XIV (P5147; MilliporeSigma) via Langendorff perfusion as previously described [15, 17]. Myocytes were stored in a modified Hank's balanced salt solution buffered with 10 mmol/liter (mM) (4-(2-hydroxyethyl)-1-piperazineethanesulfonic acid (HEPES) and supplemented with 1× essential amino acids (11130051; Thermo Fisher Scientific, Waltham, MA, USA) at room temperature. Myocytes were used 1–6 h following isolation.

Electrophysiology

Ca_v activity was recorded at room temperature using the whole-cell patch clamp technique as previously described [14, 15]. Briefly, myocytes were added to a recording chamber and bathed in a solution consisting of the following in mM: 136 NaCl, 1 $MgCl_2$, 1 $CaCl_2$, 10 glucose, 10 HEPES, 4 CsCl, 0.02 tetrodotoxin; pH 7.4. Cells were ruptured following seal formation and dialyzed (5 min) with an intracellular recording solution (in mM): 110 Cs^+ methanesulfonate, 30 CsCl, 10 HEPES, 0.5 $CaCl_2$, 2 $MgCl_2$, 5 Na_2ATP, 5 EGTA; pH 7.2. Cells were voltage clamped at −50 mV and cell size was determined by integrating the capacitance of the cell following a 25 ms, 10 mV step in voltage. Series resistance was

compensated to a minimum of 80%. Analog signals were low-pass filtered (5 kHz) then digitized (50 kHz) and voltage clamp protocols were written and executed using Clampex 10.6 (Molecular Devices, Sunnyvale, CA, USA). Leak currents were always fewer than 50 pA and were ignored.

To record I_{Ca}, cells were clamped at − 50 mV then depolarized by a series of voltage steps beginning at − 40 mV and ending at 60 mV for 1.2 s in 10-mV increments. The voltage steps were separated by 15 s. The maximum negative current at each test pulse was divided by capacitance for each cell and averaged to report the current–density/voltage relationships. The rate of fast inactivation was determined by fitting the decay portion of a current trace elicited from a test pulse to 20 mV with a bi-exponential function. To calculate conductance, the maximum negative current was divided by the driving force as described [14, 15]. The reversal potential was determined empirically for each cell and was not different between groups. Conductance/voltage relationships were fit with a single Boltzmann function as described to determine activation gating parameters [14, 15].

To measure Ca_v voltage-dependent inactivation, cells were held at − 50 mV and subjected to conditioning voltage pulses ranging from − 60 to 10 mV in 10 mV increments for 400 ms. Following the conditioning pulses, the cells were depolarized to 20 mV for 400 ms. Each sweep was separated by 15 s. The maximum negative amplitude from each current trace was normalized to the maximum negative amplitude from the first step to 20 mV. The data were fit with a single Boltzmann function as described [14, 15].

To determine the efficacy of β adrenergic activation on Ca_v activity, myocytes were clamped at -50 mV and depolarized to 10 mV every 30 s as 1 μM of the *β* adrenergic agonist isoproterenol was perfused through the recording chamber. Isoproterenol was shown to induce a hyperpolarizing shift in Ca_v activation [44]; therefore, a 10 mV test pulse was used since this was close to the saturating voltage of the GV curve (Fig. 2d) yet still elicited a measurable current from OGTKO myocytes. Current from each test pulse was normalized to the current elicited from the initial test pulse at the start of the perfusion.

Western blotting and antibodies

Total protein was isolated from OGTKO and control ventricles by homogenization in HEPES buffered saline supplemented with 1% amidosulfobentaine, 1× Complete Ultra protease inhibitor cocktail (5892970001; Roche, Mannheim, DE), 0.01 calpain inhibitors I and II (A2602 and A2603; Apex Bio, Houston, TX, USA), 0.001 thiamet G (13237; Caymen Chemical, Ann Arbor, Michigan, USA) and 0.02% Na^+ azide. In the studies investigating ubiquitination, 100 mM N-ethylmaleimide was included in the lysis buffer [18]. Protein lysates were Western blotted as previously described using a bis–tris based buffer system and gels containing an acrylamide/bis-acrylamide ratio of 49:1 to facilitate transfer of the large Ca_v α1 and α2δ1 proteins [14–17]. Immunodetection was performed using the following commercially-available antibodies: anti-Ca_v1.2, anti-Ca_vβ2, anti-Ca_vα2δ1 (ACC-003, ACC-105 and ACC-015 respectively; Alomone, Jerusalem, IL), anti-OGT, anti-mono/poly ubiquitin (24083 and 3936 respectively; Cell Signaling, Danvers, MA, USA), RL-2 (MA1-072; Thermo Fisher Scientific), anti-NEDD4-1 (611480; BD, San Jose, CA, USA), goat anti-rabbit IgG-horseradish peroxidase (HRP; AP307P; MilliporeSigma) and goat anti-mouse IgG-HRP (AP308P; MilliporeSigma). HRP signals were normalized to total protein staining by addition of 2,2,2-trichloroethanol to the resolving gel to calculate relative protein expression between OGTKO and controls as described [15, 17]. Image analysis was performed in ImageLab (Bio-Rad Laboratories, Hercules, CA, USA) and Western figures are presented as merged files consisting of the chemiluminescent and colorimetric data to show the molecular weight markers.

Whole-cell Ca^{2+} signaling and myocyte contractility measurements

LV myocytes were stained with fura-2AM and the dye was allowed to de-esterify. Stained myocytes were stimulated with 20 volts at 1 Hz (MyoPacer; IonOptix, Westwood, MA, USA) and Ca^{2+} transients were recorded ratiometrically all as previously described [15, 17]. Myocyte contraction was recorded independently by edge detection of unloaded cardiomyocytes at 250 Hz [15]; contraction was induced by stimulation as described above. Ca^{2+} signals and myocyte contraction were analyzed with FelixGX (PTI; Horiba Scientific, Edison, NJ, USA) and IonWizard 7.4 (IonOptix, Westwood, MA, USA) to compare standard parameters including max slope, time-to-peak, Ca^{2+} transient duration, activation/inactivation kinetics and fractional shortening; these parameters were calculated as the mean of ten consecutive stimulation events that followed ten unrecorded events to ensure complete SR loading. Whole-cell Ca^{2+} signals and contractility measurements were made at room temperature.

O-GlcNAc affinity precipitation

Protein was extracted as described above and preabsorbed with streptavidin coated magnetic beads (88816; Thermo Fisher Scientific) for ~ 2 h at 4 ℃. To capture proteins with the O-GlcNAc modification, biotinylated succinylated wheat germ agglutinin (sWGA; B-1025S; Vector Laboratories, Burlingame, CA, USA) was coupled to the streptavidin magnetic beads. Following preabsorption, protein was added to the lectin coupled beads and mixed overnight at 4 ℃, washed extensively with lysis buffer and eluted in 1xLDS-PAGE

sample buffer at 60 °F for 5 min. To ensure specificity, parallel experiments were always performed where sWGA was preabsorbed with 500 mM GlcNAc during the bead/lectin coupling and 50 mM during protein/bead incubations. Following elution, eluates were Western blotted as described above.

Echocardiography

Transthoracic echocardiography was performed using a Vevo 3100 (Fujifilm, Japan) equipped with a digital transducer centered on 30 MHz (20–46 MHz). Mice were anesthetized with ~ 2.0–2.5% isoflurane/O2. B and M mode images were acquired digitally and analyzed using VevoLab 3.1 (VisualSonics) to compare standard hemodynamic parameters as described by us previously [12, 15]. Briefly, 2-D mode in parasternal long axis and the parasternal short axis at the mid-papillary muscle level were imaged. From this parasternal short axis view, the 2-D guided M mode across the anterior and posterior wall were recorded and LV anterior wall thickness at diastole and systole ($LVAW_d$ and $LVAW_s$, respectively) and LV posterior wall thickness at diastole and systole ($LVPW_d$ and $LVPW_s$, respectively) were measured. Using the leading edge method, all other parameters including ejection fraction (EF) and fractional shortening (FS) were measured from three consecutive cardiac cycles according to the guidelines of the American Society of Echocardiography [40] and as described by us previously [12, 15].

Statistical analysis

Data are presented as mean ± SEM and significance was determined using unpaired student's t-tests and Mann–Whitney rank sum tests where appropriate with a p criteria of < 0.05. Animal numbers are listed as "N" and cell numbers as "n". All data are available upon request.

Results

Cardiomyocyte deletion of the OGT gene reduces OGT and O-GlcNAcylation levels by at least 90%

To assess the amount to which induced cardiomyocyte deletion of the OGT gene diminishes OGT expression, Western analysis was performed on ventricular protein lysates and indicated a nearly 90% reduction in OGTKO OGT (Fig. 1a and c; $N = 3$; $p = 0.001$). To determine the levels to which O-GlcNAcylation was reduced in OGTKO cardiomyocytes, the monoclonal antibody RL-2, which recognizes O-GlcNAcylated serine/threonine residues with only some other peptide dependence [61], was used and indicated an ~ 97% reduction in OGTKO cardiomyocyte O-GlcNAcylation (Fig. 1b and c; $N = 3$; $p = 0.001$). These results demonstrated that, following induction, OGT gene deletion markedly reduces OGT expression and cardiomyocyte O-GlcNAcylation.

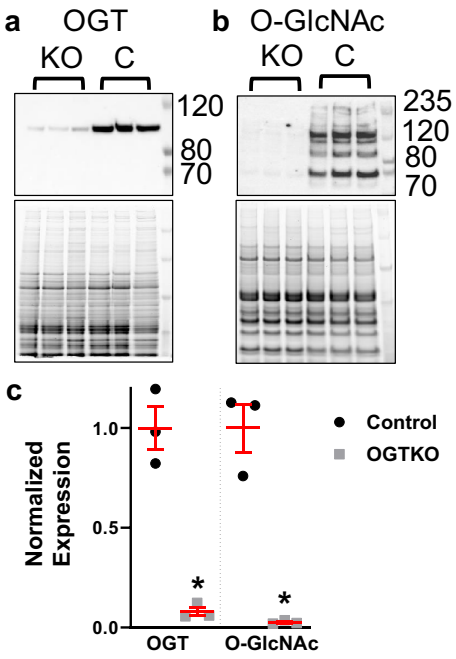

Fig. 1 Cardiomyocyte OGT-gene deletion significantly reduces OGT and O-GlcNAc levels. **a**, **b** Western and immunodetection analysis (upper panels) indicated that, following tamoxifen induction, OGTKO (KO; gray squares) ventricular OGT expression and LV myocyte O-GlcNAcylation are markedly reduced compared to controls (**c**; black circles). Signals were normalized to total protein levels (lower panels). Molecular weights in kilodaltons are listed on the right. **c** Mean ± SEM normalized OGT and O-GlcNAcylation signals ($N = 3$; $^*p = 0.001$; t-test)

Ca_v activity is diminished with chronic reductions in O-GlcNAcylation, while adrenergic efficacy is increased

To investigate whether reductions in O-GlcNAcylation affect Ca_v activity, we compared whole-cell LV cardiomyocyte I_{Ca} from OGTKO and control animals (Fig. 2a). As discussed in the Methods, here and throughout, all control animals were α-MHC-MerCreMer positive, were administered tamoxifen, but possessed a normal OGT gene; thereby, controlling for any effects of tamoxifen-treatment and Cre expression. OGTKO cardiomyocytes demonstrated significant reductions in I_{Ca} density at all channel-activating test

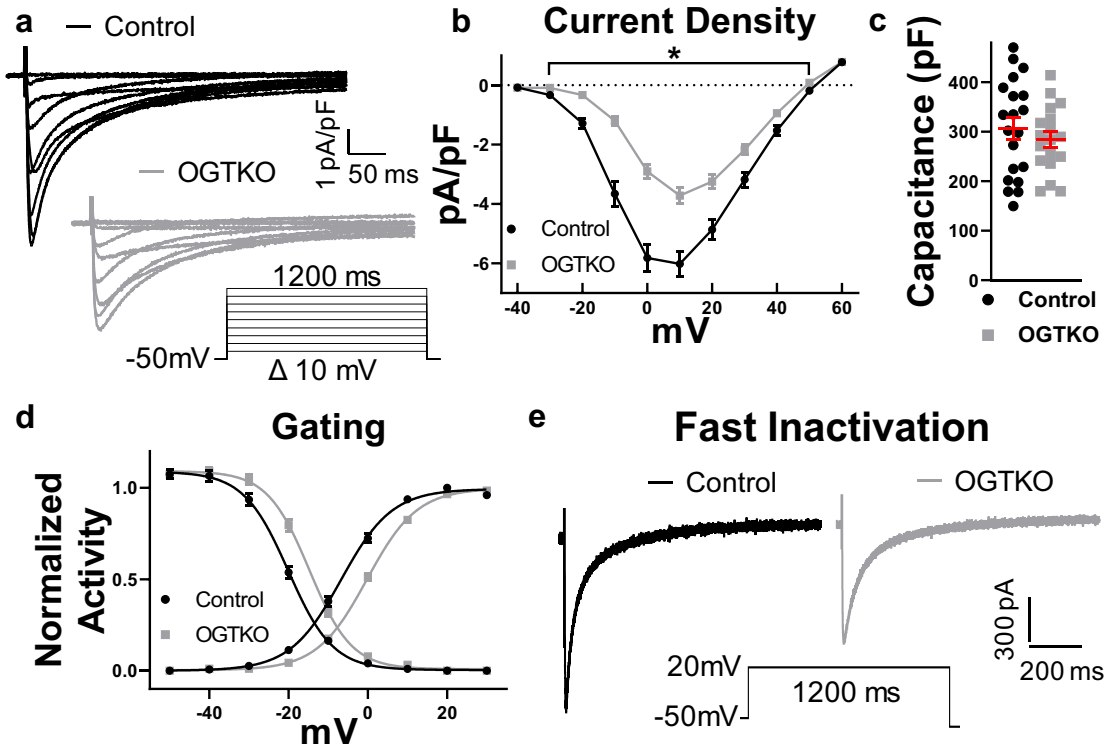

Fig. 2 Ca_v activity is diminished, gating depolarized and inactivation slowed in OGTKO LV myocytes. **a** Representative whole-cell voltage-sensitive Ca^{2+} current (I_{Ca}) density traces recorded from control (black) and OGTKO (gray) LV myocytes. **b** Current density–voltage relationships indicated significant reductions in OGTKO current densities. **c** Cell size measured as capacitance was not different between groups. **d** Ca_v voltage-dependent gating and window current were significantly depolarized by 5–6 mV in OGTKO LV myocytes. **e** The rates of the fast and slow components of Ca_v inactivation were significantly slower in OGTKO myocytes. **a**–**e** $N = 3$–4; $n = 18$–20; $^*p \leq 0.04$; *t*-test

potentials with no effect on reversal potential (Fig. 2b). For example, at a test potential of 10 mV, OGTKO I_{Ca} density was reduced by 38% compared to controls [Fig. 2b and supplemental Table 1 (ST1); $p < 0.0001$; for all I_{Ca} parameters: $N = 3$–4; $n = 18$–20]. Cell capacitances were statistically the same between groups (Fig. 2c and ST1). The voltage-dependence of Ca_v steady-state gating was determined and indicated nearly uniform depolarizing shifts of 5–6 mV for voltage-dependent inactivation and activation respectively, including rightward shifts in the activation and inactivation midpoints but with no effect on the slope of the Boltzmann fits (Fig. 2d and ST1; $p \leq 0.001$). To determine the rate of fast inactivation, current traces elicited from a 20 mV test pulse were fit with a bi-exponential function. A 20 mV test potential was utilized because this voltage occurred at a saturating point of the GV curve (Fig. 2d) so that the inherent effect of a rightward shift in voltage-dependent activation, as observed in OGTKO myocytes, would not influence the measurement of inactivation rate. Both the slow and fast components of Ca_v inactivation were significantly slower in OGTKO cardiomyocytes by 14 and 36% respectively (Fig. 2e and ST1; $p \leq 0.03$; $N = 3$–4; $n = 18$–20).

A requisite function of cardiac L-type Ca_vs is response to increased sympathetic drive through activation of cardiomyocyte adrenergic receptors resulting in increased I_{Ca} [38]. To test whether OGTKO Ca_vs respond normally to adrenergic activation, cardiomyocyte Ca_v activity was recorded before and after perfusion with 1 µM of the β-adrenergic receptor agonist isoproterenol. Myocytes were voltage-clamped at − 50 mV and depolarized to a near-saturating 10 mV test pulse every 30 s during the perfusion. Results from these experiments indicated that isoproterenol induced a robust increase in I_{Ca} in both control and OGTKO myocytes (Fig. 3e and f); however, I_{Ca} from OGTKO myocytes demonstrated a 51% larger increase following isoproterenol treatment compared to controls (Fig. 3c and ST1; ~ 1.8 versus 2.7-fold difference; $N = 3$–4; $n = 7$–8; $p = 0.02$). Despite the increased efficacy of isoproterenol on OGTKO Ca_vs, following isoproterenol treatment, OGTKO I_{Ca} was still ~ 20% lower than control I_{Ca} under basal conditions suggesting that the dysregulation of adrenergic signaling was not solely responsible for the decrease in basal OGTKO I_{Ca}.

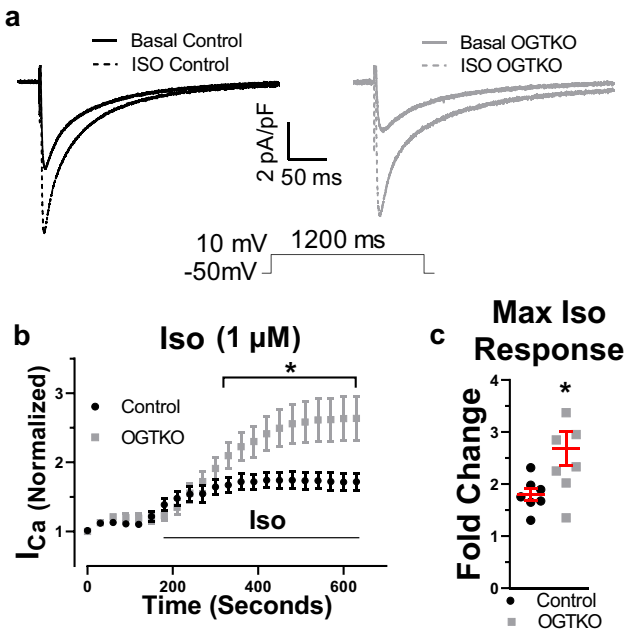

Fig. 3 The efficacy of isoproterenol on I_{Ca} is heightened in OGTKO LV myocytes. **a** Representative I_{Ca} density traces following control perfusion (basal) and perfusion with 1 μM isoproterenol (ISO). **b** Scatter plots of perfusion time with 1 μM ISO versus normalized current indicating increased efficacy of adrenergic stimulation on OGTKO Ca_v. **c** Mean ± SEM maximum fold change of I_{Ca} following perfusion with1 μM ISO. **b** and **c**: $N = 3–4$; $n = 7–8$; $^*p \leq 0.04$; *t*-test

Ca_v α1 and β2 protein levels are reduced in OGTKO hearts with α2δ1 levels unaffected

To test whether the observed reduction in OGTKO I_{Ca} density was caused by a decrease in the number of functional Ca_v, Western analysis was performed on cardiac protein lysates using antibodies that recognize the three putative cardiac Ca_v subunits. Ca_v α1 and β2 expression, but not α2δ1, were significantly reduced in OGTKO ventricles by 52 and 42% respectively (Fig. 4a–c and f; $N = 6$; $p \leq 0.0004$). Under these experimental conditions, only the truncated α1 form was detected, which was shown to represent at least 80% of the total α1 protein pool in cardiac tissue [1, 36] and can migrate in SDS-PAGE conditions through a range of apparent molecular weights (~ 175 kDa to ~ 210 kDa) largely depending on the extent of processing and the acrylamide concentration and acrylamide/bis-acrylamide ratio [11, 24, 28]. The specificities of all Ca_v subunit antibodies were tested using their respective immunizing peptides provided by the manufacturer of the antibodies.

Expression system studies previously showed that the ubiquitin ligase, neuronal precursor cell-expressed developmentally down-regulated 4 isoform 1 (NEDD4-1), down-regulates expression and activity of the L-type Ca_v [56]. It was also shown that O-GlcNAcylation negatively regulates NEDD4-1 expression [34]. We therefore rationalized that NEDD4-1 would be upregulated in OGTKO cardiomyocytes and this might contribute to the observed Ca_v downregulation. Western analysis indicated that, indeed, NEDD4-1 expression levels were 41% higher in OGTKO

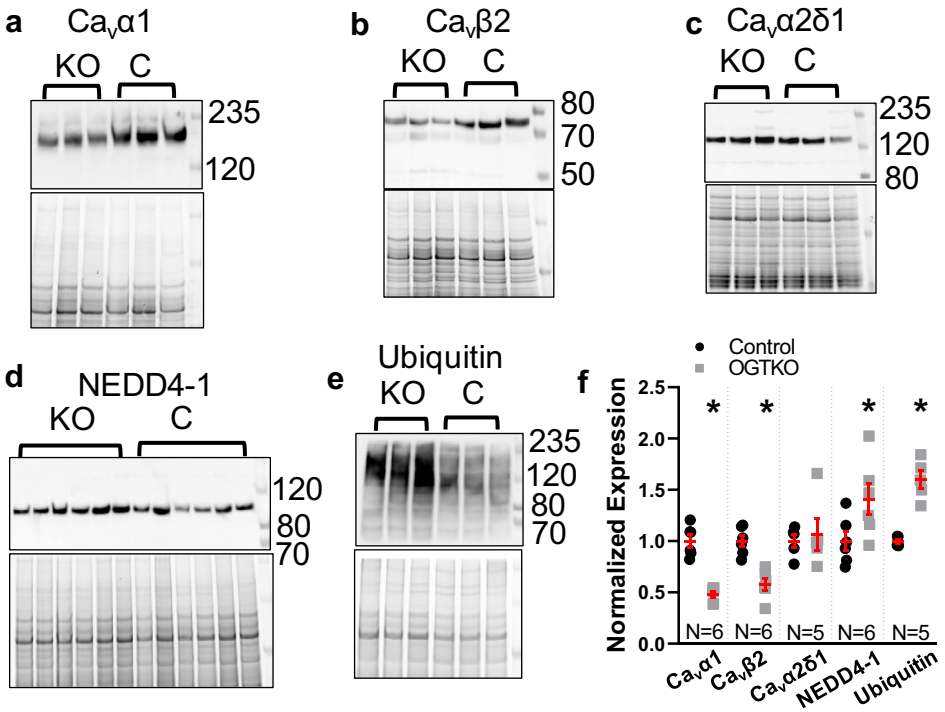

Fig. 4 Ca_v α1 and β2 expression are decreased, NEDD4-1 expression and protein ubiquitination are increased, and Ca_vα2δ1 levels are similar in OGTKO ventricles. **a**–**e** Western and immunodetection results (top panels) from OGTKO (KO; gray squares) and control (C; black circles) ventricular protein lysates. Molecular weights in kilodaltons are listed on the right. Optical densities were normalized to total protein levels (bottom panels). **f** Mean ± SEM normalized expression levels. $N = 5–6$; $^*p < 0.05$; *t*-test

hearts (Fig. 4d and f; $N=6$; $p<0.05$). A major function of NEDD4-1 is to ubiquitinate proteins which targets them for degradation [32]. While the study by Rougier et al. suggested that the regulation of L-type Ca_vs by NEDD4-1 overexpression did not involve increased $Ca_v1.2$ ubiquitination [56], interest remained in determining whether ubiquitination levels were altered in OGTKO hearts, which would be consistent with increased NEDD4-1 expression. To test this, blotted protein was subjected to immunodetection using an antibody that recognizes mono- and poly-ubiquitinated proteins; the data indicated that protein ubiquitination was increased by 60% in OGTKO hearts (Fig. 4e and f; $N=5$; $p=0.008$).

Ca_v α1 and β2 subunits are O-GlcNAcylated but the α2δ1 subunit is not

To investigate whether Ca_v subunits are directly O-GlcNAcylated, we performed affinity precipitation with biotinylated sWGA that was coupled to streptavidin-coated magnetic beads. sWGA binds terminal GlcNAc residues and can be used to precipitate O-GlcNAcylated proteins [46]. In some previous cases, affinity reagents that recognize the O-GlcNAc modification were shown to cross-react with extracellular N-glycans that possess terminal GlcNAcs [54]. Unlike here, this is often not a limitation because most proteins studied in the context of O-GlcNAcylation are nucleocytoplasmic and are typically not N-glycosylated. The $\alpha2\delta1$ subunit is heavily N-glycosylated and, while it does not appear to occur at high levels, it is possible that the cardiac $\alpha1$ subunit is N-glycosylated as well [15]; $\beta2$ is cytosolic. To overcome the potential spurious reactivity of $\alpha1$ and/or $\alpha2\delta1$ terminal N-linked GlcNAcs with sWGA, we utilized a mouse model developed by our lab where hybrid/complex N-glycosylation, and therefore the addition of terminal N-linked GlcNAcs, cannot occur (MGAT1KO) [15, 17]. Detergent soluble protein lysates from MGAT1KO hearts were subjected to sWGA precipitation and indicated that both the $\alpha1$ and $\beta2$ subunits were precipitated by sWGA while $\alpha2\delta1$ was not (Fig. 5). Similar experiments were performed using protein lysates from OGTKO and control ventricles (not shown). Precipitation of Ca_v $\alpha1$ and $\beta2$ by sWGA in control lysates was identical to that which was precipitated from MGAT1KO lysates with only marginal pull-down observed in OGTKO lysates, which was likely the result of spurious reactivity as described above, non-specific binding, and/or residual OGT expression. Together, these data, along with the functional data (Fig. 2), offer strong evidence that Ca_v $\alpha1$ and $\beta2$ are directly O-GlcNAcylated under basal conditions and that this modification is an important regulator of Ca_v function.

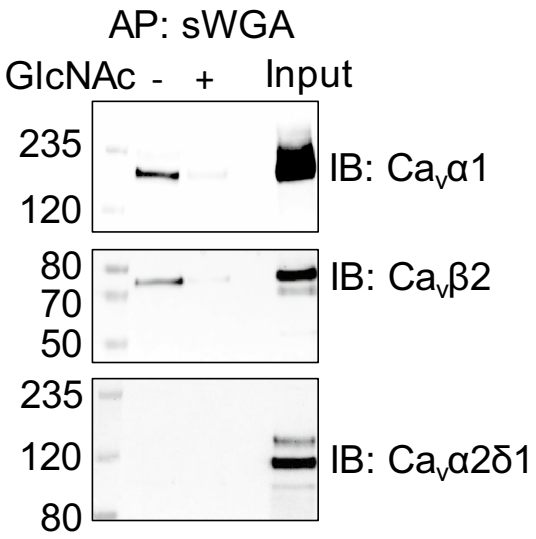

Fig. 5 Ca_v $\alpha1$ and $\beta2$ are O-GlcNAcylated but $Ca_v\alpha2\delta1$ is not. Affinity purification (AP) using the lectin sWGA, which recognizes terminal GlcNAc residues, was performed in the presence (+) or absence (−) of 500 mM N-acetylglucosamine (GlcNAc). GlcNAc was used to demonstrate specificity as free excess GlcNAc would saturate binding of the lectin and prevent precipitation of O-GlcNAcylated proteins by the bead-lectin sorbent. Precipitated protein eluates were subjected to Western and immunoblot (IB) analysis using Ca_v subunit specific antibodies and results indicated that sWGA precipitates Ca_v α1 and β2 but not Ca_v $\alpha2\delta1$. Images are representative of 5–6 independent experiments

Intracellular Ca^{2+} release and contractility are diminished and more variable in OGTKO myocytes

In cardiomyocytes, I_{Ca} is the primary trigger for release of Ca^{2+} from intracellular stores [60]. Therefore, to test whether the reductions in OGTKO Ca_v activity impact intracellular Ca^{2+} release, we performed fura-2 ratiometric Ca^{2+} photometry in field-stimulated (1 Hz/20 volts) OGTKO and control LV myocytes (Fig. 6a). OGTKO myocytes demonstrated an ~ 27% decrease in the magnitude and rate of intracellular Ca^{2+} release and a 12% slowing in the time-to-peak (TTP) of the Ca^{2+} transient (Fig. 6b–d). Contrastingly, Ca^{2+} transient duration and rate of decay, which are indicators of the time required for intracellular Ca^{2+} to be extruded or re-sequestered, were not different between groups (Fig. 6d; for all Ca^{2+} transient parameters: $N=3$; $n=43$–66; $p\leq0.003$ where significant). The robust effects on Ca^{2+} transient activation with no observed effects on Ca^{2+} transient duration or relaxation suggest that the reduction in OGTKO I_{Ca} density contributes to the diminished Ca^{2+}-activated Ca^{2+}-release observed in OGTKO LV myocytes although this does not rule out an effect of reductions in O-GlcNAc levels on ryanodine receptor activity. These data also suggest that, while phospholamban was shown to be O-GlcNAcylated [68], prevention of O-GlcNAcylation under basal conditions does

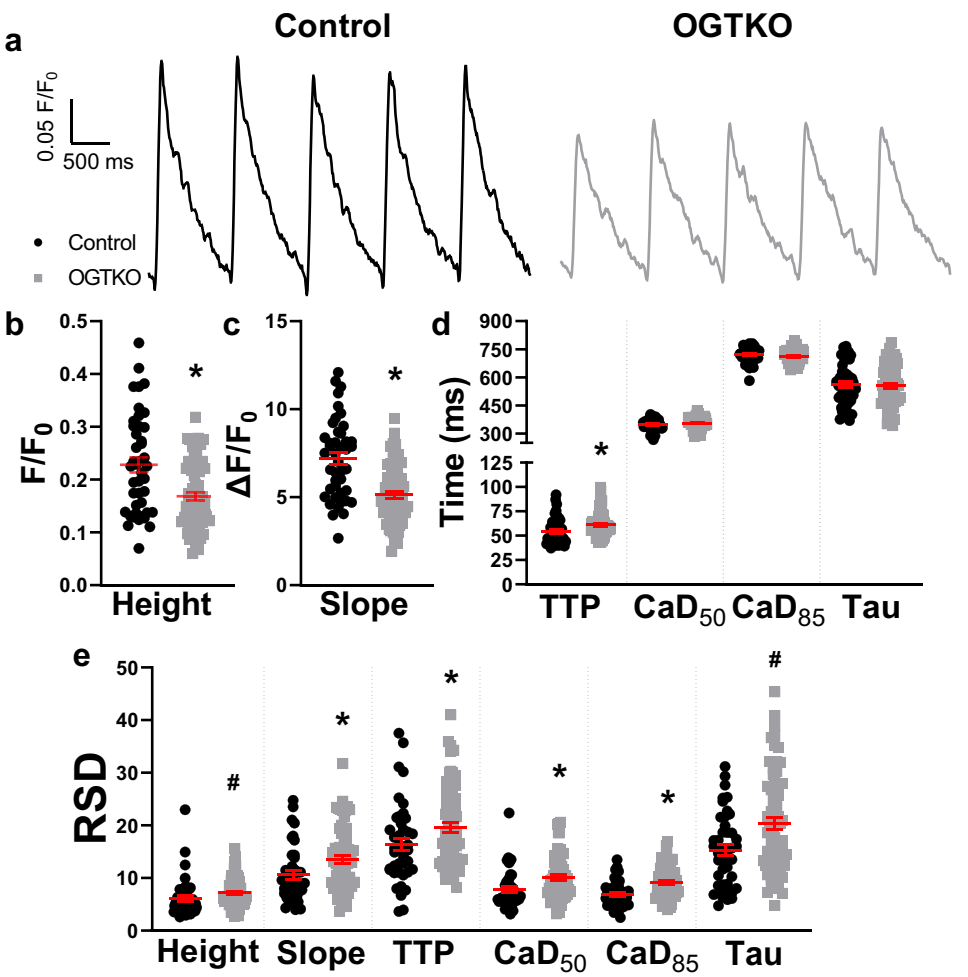

Fig. 6 The magnitude and kinetics of intracellular Ca^{2+} release are reduced and more variable in OGTKO LV myocytes with no measurable effect on Ca^{2+} re-sequestration or efflux. **a** Representative fura-2 ratiometric Ca^{2+} transients recorded from control (black) and OGTKO (gray) LV myocytes. **b**–**d** Mean ± SEM Ca^{2+} transient parameters for control (black circles) and OGTKO (gray squares) LV myocytes. **e** The relative standard deviation (RSD) of Ca^{2+} handling parameters were calculated by normalizing each parameter's standard deviation from ten consecutive Ca^{2+} transients by their respective means and indicated greater variability in OGTKO myocytes. For all Ca^{2+} handling parameters: $N = 3$; $n = 43–66$; $^{*}p \leq 0.03$, *t*-test; $^{\#}P \leq 0.009$, Mann–Whitney rank sum test. TTP: time-to-peak; $CaD_{50\text{-}85}$: Ca^{2+} transient duration at 50 and 85% return-to-baseline values; Tau: single exponential Ca^{2+} transient inactivation time constant

not measurably impact the role of phospholamban in Ca^{2+} re-sequestration.

To determine whether the decrease in OGTKO Ca^{2+}-activated Ca^{2+}-release could impact contractility, we assessed sarcomere shortening of unloaded and field stimulated (1 Hz/20 volts) LV myocytes from OGTKO and control hearts (Fig. 7a and b). Fractional shortening was significantly reduced, and the rate of shortening was slowed, each by ~ 40% in OGTKO myocytes, with no significant effect on relaxation kinetics (Fig. 7c and d; $N = 3$; $n = 18–29$; $p \leq 0.04$). In addition to the reductions in myocyte contraction, it was apparent that OGTKO fractional shortening demonstrated significantly greater beat-to-beat variability compared to controls (Fig. 7a and b). To quantify this, the relative standard deviations of ten consecutive contractions were compared between groups. Strikingly, the variability in contractile parameters from rhythmic contractions was ~ 78–177% greater in OGTKO myocytes compared to controls (Fig. 7e; $N = 3$; $n = 18–29$; $p \leq 0.02$). A similar analysis was performed on the recorded Ca^{2+} transients (Fig. 6) and while the magnitude of variability was not as large as what was observed for contractility, all OGTKO Ca^{2+} transient parameters demonstrated significantly greater variability than controls (18–33%; Fig. 6e; $N = 3$; $n = 43–66$; $p \leq 0.03$).

The deficits in OGTKO cardiomyocyte contractility are conserved at the whole-heart level

To determine whether the reductions and increased variability of myocyte Ca^{2+} handling and contractility were conserved at the whole-heart level, echocardiography of the LV was performed on OGTKO and control animals pre-induction (baseline) then again at 19 dpi (the time at which the myocyte Ca^{2+} transient and contractility measurements were made), and at 29 dpi. At 19 dpi, EF and FS were significantly reduced by ~ 37 and 45% respectively in OGTKO animals compared to baseline levels with consistent increases in end systolic volumes (ESV) and internal LV dimension at systole [($LVID_s$) Fig. 8 and ST2; $N = 7$; $p \leq 0.04$]. There were, however, no changes in wall thickness, end-diastolic volume (EDV) or internal dimensions ($LVID_d$) that would indicate hypertrophy (ST2); this is consistent with the similar OGTKO and control cell sizes as indicated through

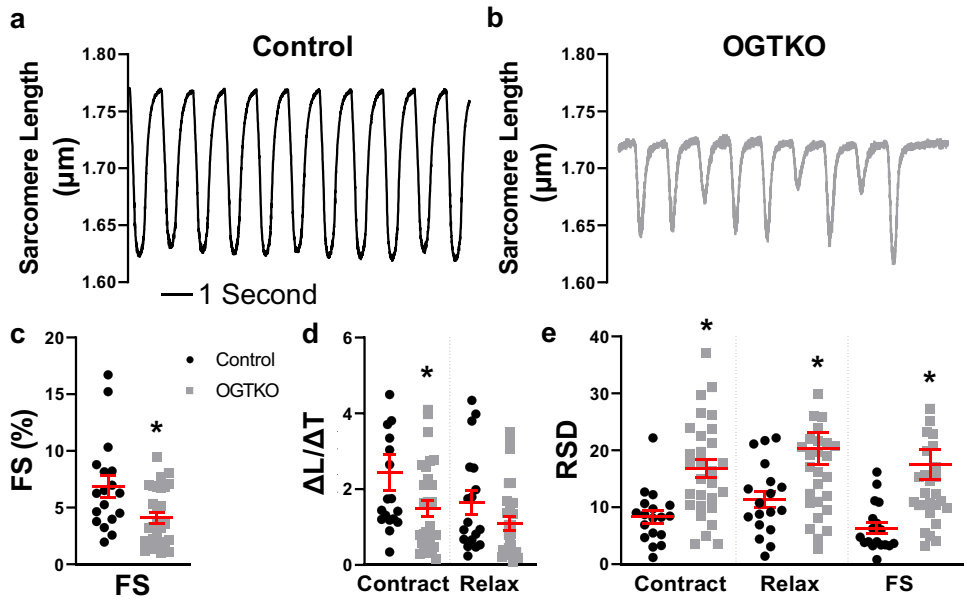

Fig. 7 OGTKO LV myocyte contractility is diminished and more variable. **a**, **b** Representative cell shortening from control (black) and OGTKO (grey) field-stimulated (20 volts/1HZ) LV myocytes. **c**, **d** Mean ± SEM fractional shortening (FS) and contraction (contract)/relaxation (relax) kinetics (change in length/time; ΔL/ΔT) for control (black circles) and OGTKO (gray squares) LV myocytes. **e** Relative standard deviation (RSD) of FS and contractile kinetics. $N = 3$; $n = 18–29$; $^{*}p \leq 0.04$; *t*-test

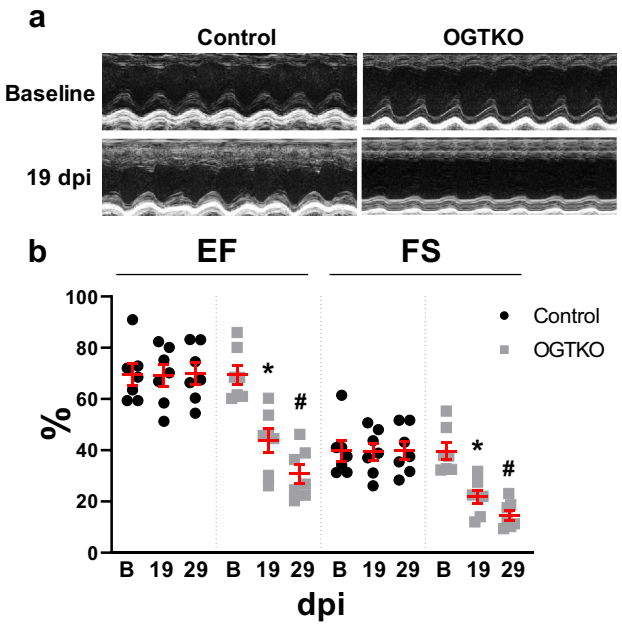

Fig. 8 OGTKO LV contractility is reduced concurrent with diminished myocyte EC coupling and worsens over time. **a** Representative M mode images taken from control (left) and OGTKO (right) left ventricles at pre-induction (baseline; top) and 19 days post induction (dpi; bottom). **b** Mean ± SEM scatter plots of LV ejection fraction (EF) and fractional shortening (FS) parameters measured from echocardiographs of control (black circles) and OGTKO (gray squares) hearts at baseline (**B**), 19 and 29 dpi. $N = 7$; $^{*}p = 0.01$: 19 dpi versus B; $^{\#}p = 0.01$: 29 dpi versus 19 dpi

membrane capacitance measurements (Fig. 2c). The loss of contractility was progressive in that at 29 dpi, OGTKO EF and FS were further reduced by ~ 30 and 33% respectively compared to 19 dpi (Fig. 8b and ST2; $N = 7$; $p = 0.01$). At 29 dpi, compared to baseline values, an ~ 23% reduction in OGTKO LVPWs was observed with no other changes in wall thicknesses (ST2; $N = 7$; $p = 0.04$) suggesting that OGTKO animals forego any hypertrophy and enter directly into heart failure. Control animals showed no significant change in any recorded parameter at any time point tested, and at baseline, all measured parameters showed no difference in systolic function between OGTKO and control hearts (Fig. 8 and ST2; $N = 7$). Together, these data strongly suggest that the EC coupling and contractile dysfunctions conferred by OGT deletion in cardiomyocytes and described in Figs. 6 and 7 translate directly to aberrant LV shortening and contractility with no indication of hypertrophy at the cellular or LV levels.

Discussion

Here we show that chronic reductions in cardiomyocyte O-GlcNAcylation significantly impact Ca_v function. We observed reductions in OGTKO I_{Ca} density, with no impact on cell size, and consistent decreases in Ca_v α1 and β2 expression. Further, the data showed increased efficacy of adrenergic stimulation on OGTKO Ca_v. We also observed rightward shifts in OGTKO Ca_v steady-state gating. Together, the data show that reduced O-GlcNAc levels impact Ca_v through at least three previously undescribed mechanisms: (1) reduced Ca_v subunit expression, (2) depolarizing shifts in Ca_v steady-state gating and window current, and (3) increased adrenergic stimulation efficacy. Furthermore, while it is not possible at this time to rule out a contribution of aberrant contractile protein function, some of which were shown to be dynamically O-GlcNAcylated [52,

53], or dysregulation of intracellular Ca^{2+} handling proteins, the observed reductions and increased variability in Ca^{2+} handling and contractility are consistent with reduced and altered Ca_v function including the observed rightward shift in OGTKO Ca_v window current and slowing of inactivation (Fig. 2d and e) suggesting a critical role for O-GlcNAcylation in these processes. Finally, the severe impact of OGT gene deletion on cardiomyocyte EC coupling is observed at the whole-heart level as evidenced by the concurrent and progressive loss of OGTKO LV contractility (Fig. 8) in the absence of hypertrophy.

Increased NEDD4-1 and protein ubiquitination in the OGTKO are consistent with decreased Ca_v expression and I_{Ca}

Work by Rougier et al. suggested that NEDD4-1 overexpression regulates L-type Ca_vs by disrupting the exit of Ca_vs from the Golgi [56]. Here, studies into a potential role of endogenous NEDD4-1 in reducing OGTKO Ca_v activity and subunit expression indicated that NEDD4-1 levels and protein ubiquitination are elevated in OGTKO ventricles (Fig. 4d–f) but a direct relationship between these phenomena and the reduction in OGTKO Ca_vs has yet to be established. O-GlcNAcylation was specifically shown to limit protein degradation by blocking ubiquitination [42]; therefore, it is reasonable to predict increased ubiquitination in the absence of OGT. Studies investigating whether OGTKO Ca_v are retained in the Golgi or demonstrate differences in ubiquitination or interactions with ubiquitin-related proteins are currently ongoing but are, as of yet, inconclusive. A subsequent study by the same group also identified the deubiquitinating (dub) enzyme USP2 as a negative regulator of L-type Ca_vs [57] and O-GlcNAcylation was shown by other groups to regulate several dub proteins [58]. Dub proteins and ubiquitin ligases such as NEDD4-1 serve antagonizing roles in the ubiquitination process; thus, it is surprising that such proteins would have similar effects on Ca_v activity/expression. Although it is important to point out that the studies investigating the impact of NEDD4-1 and USP2 on the L-type Ca_v were performed in over-expression systems that likely do not recapitulate a native cardiomyocyte. The regulation of membrane proteins through ubiquitination and, ultimately, degradation is critically important as well as being exceedingly complex involving thousands of proteins [21]. Whether and how O-GlcNAcylation regulates ventricular myocyte Ca_v expression, and thereby I_{Ca} density, through an interplay with ubiquitination will require additional work; however, it is clear that OGT-gene deletion and, presumably, the subsequent reductions in O-GlcNAcylation, impact ubiquitin signaling as evidenced by the significant increase in ubiquitinated proteins in OGTKO hearts (Fig. 4e and f) suggesting an important link between these processes.

Potential mechanisms by which reduced O-GlcNAcylation impacts Ca_v gating and results in increased adrenergic stimulation efficacy

While alterations in the OGTKO NEDD4-1/ubiquitin pathway may well explain the reduced I_{Ca} density and Ca_v subunit expression levels, it is unlikely that this pathway can explain the additional observation of a rightward shift in OGTKO Ca_v steady-state-gating and window current or slowing of inactivation. Thus, we initially hypothesized that the depolarization of steady-state gating was caused through electrostatic mechanisms conferred by an increase in Ca_v subunit phosphorylation in the OGTKO. This speculation was based on the fact that O-GlcNAcylation often overlaps with phosphorylation where the same serine/threonine residue can be reciprocally modified [30] and cardiac Ca_v α1 and β2 subunits are substrates of several kinases [23, 25, 51], and, as reported here for the first time, are O-GlcNAcylated under basal conditions in ventricular myocytes (Fig. 5). Thus, it is conceivable to infer conservation of the two modifications among some α1 and β2 serine/threonine residues. Based on this, we rationalized that, in the absence of O-GlcNAcylation in OGTKO cardiomyocytes, the O-GlcNAcylation/phosphorylation equilibrium of Ca_v α1 and β2 would shift toward increased phosphorylation. The impact of phosphorylation on cardiac Ca_v function can vary greatly depending on the kinases involved and the Ca_v subunits and residues that are phosphorylated with both increases and decreases in Ca_v activity being reported as well as rightward and leftward shifts in gating [7, 35, 37]. As one example, a phosphomimetic mutation in Ca_v β2 resulted in a decrease in Ca_v activity and a marked rightward shift in activation and inactivation gating [7]. However, we speculate that if increased Ca_v phosphorylation in the OGTKO contributes to the effect of reduced O-GlcNAcylation on Ca_v gating, it may not occur through any one specific phosphorylation pathway, but rather through a non-specific electrostatic mechanism. That is, as suggested by others [3, 27], a general increase in the number of negatively charged phosphate groups attached to the cytosolic portions of OGTKO Ca_v subunits, or other proteins in sufficiently close proximity, may effectively hyperpolarize the membrane potential sensed by the Ca_v voltage sensors, thereby requiring a greater depolarization for OGTKO Ca_v gating to occur as is observed (Fig. 2d). An investigation into the role of increased Ca_v phosphorylation in conditions of reduced O-GlcNAcylation and how this may impact channel function utilizing proteomic and pharmacologic approaches is necessary and ongoing. To this end, identifying the specific Ca_v $\alpha 1$ and $\beta 2$ residues that are O-GlcNAcylated and the phosphorylation pathways that are disrupted in the OGTKO will be of paramount

importance in resolving these questions. Alterations in Ca_v phosphorylation or signaling pathways that utilize phosphorylation may also contribute to the slowing of OGTKO Ca_v inactivation (Fig. 2e). However, because Ca^{2+} influx accelerates Ca_v inactivation [Ca^{2+}-dependent inactivation (CDI) [41]], under these experimental conditions, it is difficult to speculate a cause of the slowing of OGTKO Ca_v inactivation other than simply due to the reduced current (and thereby, reduced CDI). This is supported by the fact that the fast component of inactivation, which is largely thought to be ascribed to CDI [26], is impacted to a greater degree (~ 36% versus 14%; Fig. 2e and ST1) in OGTKO cardiomyocytes. This does not, however, rule out a direct effect on calmodulin, which is the Ca^{2+} sensor in CDI [49]. Additional experiments utilizing different intracellular Ca^{2+} concentrations and chelators or charge carriers (e.g., Ba^{2+}) will be required to explore this phenomenon more rigorously. Irrespective of the precise mechanism, the uniform rightward shifts in OGTKO Ca_v voltage-dependent steady-state gating and window current and the slowing of inactivation would be expected to confer a complex set of gains and losses of Ca_v function that would alter intracellular Ca^{2+} dynamics and, potentially, action potential duration [2]; these effects are all consistent with the significantly increased variability of EC coupling observed in OGTKO LV myocytes (Figs. 6e, 7a, b and e).

In addition to an interplay with ubiquitination and phosphorylation, O-GlcNAcylation was shown to affect protein function by modulating protein-to-protein interactions [67]. Therefore, an additional possible explanation for the reduction in OGTKO Ca_v activity and the shift in gating may stem from a disruption in the Ca_v complex, which could impact the stability of the channel. Additionally, evidence suggests an indispensable role for Rad, which is a member of the Rad and Gem/Kir Ras-related GTP-binding protein (RGK) family, in the regulation of cardiomyocyte Ca_v function. Under basal conditions, Rad inhibits Ca_v activity and, during adrenergic stimulation, Rad dissociates from Ca_vs removing its tonic inhibition [44]. Cardiomyocyte-specific deletion of the Rad gene resulted in an increase in Ca_v activity and a hyperpolarizing shift in activation gating [47]. Several RGK proteins are regulated by O-GlcNAcylation [43, 66], thus, given the data provided here, it is interesting to speculate a potential role for the regulation of Ca_vs by O-GlcNacylation that is mediated through Rad. If, for example, reductions in O-GlcNAcylation affect the expression of Rad or interaction of Rad with Ca_vs while also making Rad more susceptible to PKA phosphorylation during adrenergic stimulation, this could explain the effect of OGT gene deletion on Ca_v activity including the increased efficacy of adrenergic stimulation (Fig. 3). Preliminary studies into whether Rad expression is altered in the OGTKO and whether it is O-GlcNAcylated have been hampered by the lack of a suitable Rad antibody but are ongoing.

Potential pathophysiologic effects of altered O-GlcNAcylation on cardiac function

The reduction in OGTKO Ca_v activity was surprising in that some of the impetus for these studies was predicated on the fact that experimental models of diabetes/hyperglycemia were shown to result in reduced cardiomyocyte L-type Ca_v activity, with mechanisms largely unknown [45, 48, 63], while increased O-GlcNAcylation was shown to contribute to the pathologic molecular remodeling associated with diabetes [9, 19, 31, 50, 52, 53, 68]. An initial hypothesis, therefore, was that OGTKO Ca_v activity would be increased. If increased O-GlcNAcylation is involved in the reduction of Ca_v activity in diabetic models, there are several possible explanations for the apparent discrepancies between previous disease-related studies and our data here. As one example, there may be a multi-phasic effect of O-GlcNAc signaling on Ca_v activity in conditions of hyperglycemia. Others have also shown a protective effect of increased O-GlcNAcylation on cardiac function in that acute increases in O-GlcNAcylation, caused by the release of an unidentified humoral factor during a remote ischemic preconditioning intervention (rIPC), contributed to improved restoration of contractility following ischemia reperfusion injury [33]. Interestingly, the group also showed that diabetic patients, for whom O-GlcNAc levels would likely be higher under basal conditions due to the diabetes-related hyperglycemia, offered similar cardioprotection before rIPC but no additional protection after rIPC [33]. More specific models that link hyperglycemia, temporal increases in O-GlcNAcylation, and Ca_v function will be required to investigate these phenomena more rigorously. Pointedly, however, results from this study indicate that O-GlcNAcylation is a critical and direct regulator of cardiac Ca_v function; therefore, it is likely that in this model, where cardiomyocyte O-GlcNAcylation is drastically reduced and O-GlcNAc homeostasis is disrupted, a more severe phenotype is observed which is not fully reflective of diabetic/hyperglycemic disease-states where changes in O-GlcNAcylation would likely be more subtle and/or transient. Nevertheless, in addition to providing the first insight into this novel form of cardiac L-type Ca_v regulation, use of the OGTKO model, along with the development of more refined models that target individual Ca_v α1 and β2 O-GlcNAcylation sites, should prove invaluable in elucidating the role of O-GlcNAcylation in mediating the effects of various signaling pathways that modulate Ca_v function in health and disease. Additionally, determining the impact of more transient changes in O-GlcNAc levels on Ca_v function should help uncover

how O-GlcNAcylation regulates Ca_v activity under basal conditions. Initial studies using glucosamine or OGA inhibitors, both of which can acutely increase O-GlcNAc levels, on isolated cardiomyocytes (1–6 h), indicated that such an approach is ineffective in modulating Ca_v function although this may be due to an inability to incubate adult mouse cardiomyocytes for a sufficient duration that alters Ca_v O-GlcNAcylation yet still allows for reliable I_{Ca} recordings.

It was previously shown in a similar model that ablation of the OGT-gene in adult mouse cardiomyocytes depressed cardiac function in non-stressed animals as evidenced by significantly reduced EF that onsets at approximately 4 weeks of age [65, 69]. Here we show that the deficits in OGTKO cardiac contractility (EF and to a larger extent FS) onset even earlier (19 dpi) with no indications of hypertrophy at the LV or myocyte levels (Figs. 2c and 8 and ST1 and ST2). Additionally, our data, as well as those from others, indicate that the reductions in ventricular contractility worsen over time along with an increase in systolic volume by 29 dpi (ST2) and an increase in diastolic volume by 2 months [65] suggesting dilation. Inducible cardiomyocyte OGT ablation was also shown to exacerbate the functional deterioration observed in pressure-overload and infarct models [10, 64, 69]. Several lines of questioning were investigated without identifying a causative mechanism. Our data here indicate for the first time that OGTKO LV myocyte Ca_v activity, intracellular Ca^{2+} release and contractility are all markedly reduced (Figs. 2, 6 and 7) by as early as 18 dpi (the earliest time-point tested). These data, therefore, suggest that diminished OGTKO cardiomyocyte EC coupling, largely resulting from a direct reduction in L-type Ca_v activity, plays a major role in the development of heart disease that likely progresses to heart failure, thus highlighting the critical role of O-GlcNAcylation in these processes as well as in the function of healthy and diseased hearts.

Funding This work was supported in part by grants from the National Science Foundation [Division of Molecular and Cellular Biosciences-1856199 to A.R.E and E.S.B., Division of Integrative Organismal Systems-1660926 to E.S.B.]; an American Heart Association Postdoctoral Fellowship (15POST25710010 to A.R.E]; and an American Heart Association Greater Southeast Affiliate Grant-In-Aid [14GRNT20450148 to E.S.B.].

Availability of data and materials All data and materials are available upon request.

Compliance with ethical standard

Conflict of interest The authors declare that they have no conflict of interest or competing interests.

Ethics approval Animals were handled in accordance with the NIH Guide for the Care and Use of Laboratory Animals. All protocols involving animals were approved by the Wright State University Institutional Animal Care and Use Committee (AUP 1163).

Consent to participate Not applicable.

Consent for publication All authors freely consent for publication.

Code availability Not applicable.

References

1. Abele K, Yang J (2012) Regulation of voltage-gated calcium channels by proteolysis. Sheng Li Xue Bao 64:504–514
2. Alseikhan BA, DeMaria CD, Colecraft HM, Yue DT (2002) Engineered calmodulins reveal the unexpected eminence of Ca2 + channel inactivation in controlling heart excitation. Proc Natl Acad Sci U S A. 99:17185–17190. https://doi.org/10.1073/pnas.262372999
3. Ariyaratne A, Zocchi G (2015) Artificial phosphorylation sites modulate the activity of a voltage-gated potassium channel. Phys Rev E Stat Nonlin Soft Matter Phys. 91:032701. https://doi.org/10.1103/physreve.91.032701
4. Banerjee PS, Ma J, Hart GW (2015) Diabetes-associated dysregulation of O-GlcNAcylation in rat cardiac mitochondria. Proc Natl Acad Sci U S A. 112:6050–6055. https://doi.org/10.1073/pnas.1424017112
5. Bers DM, Grandi E (2009) Calcium/calmodulin-dependent kinase II regulation of cardiac ion channels. J Cardiovasc Pharmacol 54:180–187. https://doi.org/10.1097/FJC.0b013e3181a25078
6. Bersell K, Choudhury S, Mollova M, Polizzotti BD, Ganapathy B, Walsh S, Wadugu B, Arab S, Kuhn B (2013) Moderate and high amounts of tamoxifen in alphaMHC-MerCreMer mice induce a DNA damage response, leading to heart failure and death. Dis Model Mech. 6:1459–1469. https://doi.org/10.1242/dmm.010447
7. Brunet S, Emrick MA, Sadilek M, Scheuer T, Catterall WA (2015) Phosphorylation sites in the Hook domain of CaVbeta subunits differentially modulate CaV1.2 channel function. J Mol Cell Cardiol 87:248–256. https://doi.org/10.1016/j.yjmcc.2015.08.006
8. Bugger H, Abel ED (2014) Molecular mechanisms of diabetic cardiomyopathy. Diabetologia 57:660–671. https://doi.org/10.1007/s00125-014-3171-6
9. Clark RJ, McDonough PM, Swanson E, Trost SU, Suzuki M, Fukuda M, Dillmann WH (2003) Diabetes and the accompanying hyperglycemia impairs cardiomyocyte calcium cycling through increased nuclear O-GlcNAcylation. J Biol Chem 278:44230–44237. https://doi.org/10.1074/jbc.M303810200
10. Dassanayaka S, Brainard RE, Watson LJ, Long BW, Brittian KR, DeMartino AM, Aird AL, Gumpert AM, Audam TN, Kilfoil PJ, Muthusamy S, Hamid T, Prabhu SD, Jones SP (2017) Cardiomyocyte Ogt limits ventricular dysfunction in mice following pressure overload without affecting hypertrophy. Basic Res Cardiol 112:23. https://doi.org/10.1007/s00395-017-0612-7
11. De Jongh KS, Warner C, Colvin AA, Catterall WA (1991) Characterization of the two size forms of the alpha 1 subunit of skeletal muscle L-type calcium channels. Proc Natl Acad Sci U S A. 88:10778–10782. https://doi.org/10.1073/pnas.88.23.10778
12. Deng W, Ednie AR, Qi J, Bennett ES (2016) Aberrant sialylation causes dilated cardiomyopathy and stress-induced heart failure. Basic Res Cardiol 111:57. https://doi.org/10.1007/s00395-016-0574-1
13. Dubois-Deruy E, Belliard A, Mulder P, Bouvet M, Smet-Nocca C, Janel S, Lafont F, Beseme O, Amouyel P, Richard V, Pinet F (2015) Interplay between troponin T phosphorylation and

O-N-acetylglucosaminylation in ischaemic heart failure. Cardiovasc Res 107:56–65. https://doi.org/10.1093/cvr/cvv136
14. Ednie AR, Bennett ES (2015) Reduced sialylation impacts ventricular repolarization by modulating specific K + channel isoforms distinctly. J Biol Chem 290:2769–2783. https://doi.org/10.1074/jbc.M114.605139
15. Ednie AR, Deng W, Yip KP, Bennett ES (2019) Reduced myocyte complex N-glycosylation causes dilated cardiomyopathy. FASEB J. 33:1248–1261. https://doi.org/10.1096/fj.201801057R
16. Ednie AR, Horton KK, Wu J, Bennett ES (2013) Expression of the sialyltransferase, ST3Gal4, impacts cardiac voltage-gated sodium channel activity, refractory period and ventricular conduction. J Mol Cell Cardiol 59:117–127. https://doi.org/10.1016/j.yjmcc.2013.02.013
17. Ednie AR, Parrish AR, Sonner MJ, Bennett ES (2019) Reduced hybrid/complex N-glycosylation disrupts cardiac electrical signaling and calcium handling in a model of dilated cardiomyopathy. J Mol Cell Cardiol 132:13–23. https://doi.org/10.1016/j.yjmcc.2019.05.001
18. Emmerich CH, Cohen P (2015) Optimising methods for the preservation, capture and identification of ubiquitin chains and ubiquitylated proteins by immunoblotting. Biochem Biophys Res Commun 466:1–14. https://doi.org/10.1016/j.bbrc.2015.08.109
19. Erickson JR, Pereira L, Wang L, Han G, Ferguson A, Dao K, Copeland RJ, Despa F, Hart GW, Ripplinger CM, Bers DM (2013) Diabetic hyperglycaemia activates CaMKII and arrhythmias by O-linked glycosylation. Nature 502:372–376. https://doi.org/10.1038/nature12537
20. Facundo HT, Brainard RE, Watson LJ, Ngoh GA, Hamid T, Prabhu SD, Jones SP (2012) O-GlcNAc signaling is essential for NFAT-mediated transcriptional reprogramming during cardiomyocyte hypertrophy. Am J Physiol Heart Circ Physiol. 302:H2122–2130. https://doi.org/10.1152/ajpheart.00775.2011
21. Foot N, Henshall T, Kumar S (2017) Ubiquitination and the Regulation of Membrane Proteins. Physiol Rev 97:253–281. https://doi.org/10.1152/physrev.00012.2016
22. Fu Y, Xiao H, Zhang Y (2012) Beta-adrenoceptor signaling pathways mediate cardiac pathological remodeling. Front Biosci (Elite Ed) 4:1625–1637. https://doi.org/10.2741/484
23. Fuller MD, Emrick MA, Sadilek M, Scheuer T, Catterall WA (2010) Molecular mechanism of calcium channel regulation in the fight-or-flight response. Sci Signal 3:ra70. https://doi.org/10.1126/scisignal.2001152
24. Gao T, Puri TS, Gerhardstein BL, Chien AJ, Green RD, Hosey MM (1997) Identification and subcellular localization of the subunits of L-type calcium channels and adenylyl cyclase in cardiac myocytes. J Biol Chem 272:19401–19407. https://doi.org/10.1074/jbc.272.31.19401
25. Gerhardstein BL, Puri TS, Chien AJ, Hosey MM (1999) Identification of the sites phosphorylated by cyclic AMP-dependent protein kinase on the beta 2 subunit of L-type voltage-dependent calcium channels. Biochemistry 38:10361–10370. https://doi.org/10.1021/bi990896o
26. Grandi E, Morotti S, Ginsburg KS, Severi S, Bers DM (2010) Interplay of voltage and Ca-dependent inactivation of L-type Ca current. Prog Biophys Mol Biol 103:44–50. https://doi.org/10.1016/j.pbiomolbio.2010.02.001
27. Green WN, Andersen OS (1991) Surface charges and ion channel function. Annu Rev Physiol 53:341–359. https://doi.org/10.1146/annurev.ph.53.030191.002013
28. Haase H, Striessnig J, Holtzhauer M, Vetter R, Glossmann H (1991) A rapid procedure for the purification of cardiac 1,4-dihydropyridine receptors from porcine heart. Eur J Pharmacol 207:51–59. https://doi.org/10.1016/s0922-4106(05)80037-9
29. Hart GW (2014) Three decades of research on O-GlcNAcylation—a major nutrient sensor that regulates signaling, transcription and cellular metabolism. Front Endocrinol. (Lausanne) 5:183. https://doi.org/10.3389/fendo.2014.00183
30. Hart GW, Slawson C, Ramirez-Correa G, Lagerlof O (2011) Cross talk between O-GlcNAcylation and phosphorylation: roles in signaling, transcription, and chronic disease. Annu Rev Biochem 80:825–858. https://doi.org/10.1146/annurev-biochem-060608-102511
31. Hu Y, Belke D, Suarez J, Swanson E, Clark R, Hoshijima M, Dillmann WH (2005) Adenovirus-mediated overexpression of O-GlcNAcase improves contractile function in the diabetic heart. Circ Res 96:1006–1013. https://doi.org/10.1161/01.Res.0000165478.06813.58
32. Ingham RJ, Gish G, Pawson T (2004) The Nedd4 family of E3 ubiquitin ligases: functional diversity within a common modular architecture. Oncogene 23:1972–1984. https://doi.org/10.1038/sj.onc.1207436
33. Jensen RV, Zachara NE, Nielsen PH, Kimose HH, Kristiansen SB, Bøtker HE (2013) Impact of O-GlcNAc on cardioprotection by remote ischaemic preconditioning in non-diabetic and diabetic patients. Cardiovasc Res 97:369–378. https://doi.org/10.1093/cvr/cvs337
34. Jiang K, Bai B, Ta Y, Zhang T, Xiao Z, Wang PG, Zhang L (2016) O-GlcNAc regulates NEDD4-1 stability via caspase-mediated pathway. Biochem Biophys Res Commun 471:539–544. https://doi.org/10.1016/j.bbrc.2016.02.037
35. Kamp TJ, Hell JW (2000) Regulation of cardiac L-type calcium channels by protein kinase A and protein kinase C. Circ Res 87:1095–1102. https://doi.org/10.1161/01.res.87.12.1095
36. Katchman A, Yang L, Zakharov SI, Kushner J, Abrams J, Chen BX, Liu G, Pitt GS, Colecraft HM, Marx SO (2017) Proteolytic cleavage and PKA phosphorylation of alpha1C subunit are not required for adrenergic regulation of CaV1.2 in the heart. Proc Natl. Acad Sci U S A. 114:9194–9199. https://doi.org/10.1073/pnas.1706054114
37. Keef KD, Hume JR, Zhong J (2001) Regulation of cardiac and smooth muscle Ca(2+) channels (Ca(V)1.2a, b) by protein kinases. Am J Physiol Cell Physiol 281:C1743–1756. https://doi.org/10.1152/ajpcell.2001.281.6.C1743
38. Kumari N, Gaur H, Bhargava A (2018) Cardiac voltage gated calcium channels and their regulation by beta-adrenergic signaling. Life Sci 194:139–149. https://doi.org/10.1016/j.lfs.2017.12.033
39. Laczy B, Marsh SA, Brocks CA, Wittmann I, Chatham JC (2010) Inhibition of O-GlcNAcase in perfused rat hearts by NAG-thiazolines at the time of reperfusion is cardioprotective in an O-GlcNAc-dependent manner. Am J Physiol Heart Circ Physiol. 299:H1715–1727. https://doi.org/10.1152/ajpheart.00337.2010
40. Lang RM, Badano LP, Mor-Avi V, Afilalo J, Armstrong A, Ernande L, Flachskampf FA, Foster E, Goldstein SA, Kuznetsova T, Lancellotti P, Muraru D, Picard MH, Rietzschel ER, Rudski L, Spencer KT, Tsang W, Voigt JU (2015) Recommendations for cardiac chamber quantification by echocardiography in adults: an update from the American Society of Echocardiography and the European Association of Cardiovascular Imaging. J Am Soc Echocardiogr 28:1–39.e14. https://doi.org/10.1016/j.echo.2014.10.003
41. Lee KS, Marban E, Tsien RW (1985) Inactivation of calcium channels in mammalian heart cells: joint dependence on membrane potential and intracellular calcium. J Physiol 364:395–411. https://doi.org/10.1113/jphysiol.1985.sp015752
42. Li MD, Ruan HB, Hughes ME, Lee JS, Singh JP, Jones SP, Nitabach MN, Yang X (2013) O-GlcNAc signaling entrains the circadian clock by inhibiting BMAL1/CLOCK ubiquitination. Cell Metab 17:303–310. https://doi.org/10.1016/j.cmet.2012.12.015
43. Lima VV, Giachini FR, Hardy DM, Webb RC, Tostes RC (2011) O-GlcNAcylation: a novel pathway contributing to the effects of endothelin in the vasculature. Am J Physiol Regul Integr Comp

Physiol 300:R236–250. https://doi.org/10.1152/ajpregu.00230.2010
44. Liu G, Papa A, Katchman AN, Zakharov SI, Roybal D, Hennessey JA, Kushner J, Yang L, Chen BX, Kushnir A, Dangas K, Gygi SP, Pitt GS, Colecraft HM, Ben-Johny M, Kalocsay M, Marx SO (2020) Mechanism of adrenergic CaV1.2 stimulation revealed by proximity proteomics. Nature 577:695–700. https://doi.org/10.1038/s41586-020-1947-z
45. Lu Z, Ballou LM, Jiang YP, Cohen IS, Lin RZ (2011) Restoration of defective L-type Ca2+ current in cardiac myocytes of type 2 diabetic db/db mice by Akt and PKC-iota. J Cardiovasc Pharmacol 58:439–445. https://doi.org/10.1097/FJC.0b013e318228e68c
46. Luo B, Soesanto Y, McClain DA (2008) Protein modification by O-linked GlcNAc reduces angiogenesis by inhibiting Akt activity in endothelial cells. Arterioscler Thromb Vasc Biol 28:651–657. https://doi.org/10.1161/atvbaha.107.159533
47. Manning JR, Yin G, Kaminski CN, Magyar J, Feng HZ, Penn J, Sievert G, Thompson K, Jin JP, Andres DA, Satin J (2013) Rad GTPase deletion increases L-type calcium channel current leading to increased cardiac contraction. J Am Heart Assoc 2:e000459. https://doi.org/10.1161/jaha.113.000459
48. Pereira L, Matthes J, Schuster I, Valdivia HH, Herzig S, Richard S, Gomez AM (2006) Mechanisms of [Ca2+]i transient decrease in cardiomyopathy of db/db type 2 diabetic mice. Diabetes 55:608–615. https://doi.org/10.2337/diabetes.55.03.06.db05-1284
49. Peterson BZ, DeMaria CD, Adelman JP, Yue DT (1999) Calmodulin is the Ca2+ sensor for Ca2+ -dependent inactivation of L-type calcium channels. Neuron 22:549–558. https://doi.org/10.1016/s0896-6273(00)80709-6
50. Peterson SB, Hart GW (2016) New insights: a role for O-GlcNAcylation in diabetic complications. Crit Rev Biochem Mol Biol 51:150–161. https://doi.org/10.3109/10409238.2015.1135102
51. Puri TS, Gerhardstein BL, Zhao XL, Ladner MB, Hosey MM (1997) Differential effects of subunit interactions on protein kinase A- and C-mediated phosphorylation of L-type calcium channels. Biochemistry 36:9605–9615. https://doi.org/10.1021/bi970500d
52. Ramirez-Correa GA, Jin W, Wang Z, Zhong X, Gao WD, Dias WB, Vecoli C, Hart GW, Murphy AM (2008) O-linked GlcNAc modification of cardiac myofilament proteins: a novel regulator of myocardial contractile function. Circ Res 103:1354–1358. https://doi.org/10.1161/circresaha.108.184978
53. Ramirez-Correa GA, Ma J, Slawson C, Zeidan Q, Lugo-Fagundo NS, Xu M, Shen X, Gao WD, Caceres V, Chakir K, DeVine L, Cole RN, Marchionni L, Paolocci N, Hart GW, Murphy AM (2015) Removal of abnormal myofilament O-GlcNAcylation restores Ca2+ sensitivity in diabetic cardiac muscle. Diabetes 64:3573–3587. https://doi.org/10.2337/db14-1107
54. Reeves RA, Lee A, Henry R, Zachara NE (2014) Characterization of the specificity of O-GlcNAc reactive antibodies under conditions of starvation and stress. Anal Biochem 457:8–18. https://doi.org/10.1016/j.ab.2014.04.008
55. Ren J, Gintant GA, Miller RE, Davidoff AJ (1997) High extracellular glucose impairs cardiac E-C coupling in a glycosylation-dependent manner. Am J Physiol 273:H2876–2883. https://doi.org/10.1152/ajpheart.1997.273.6.H2876
56. Rougier JS, Albesa M, Abriel H, Viard P (2011) Neuronal precursor cell-expressed developmentally down-regulated 4-1 (NEDD4-1) controls the sorting of newly synthesized Ca(V)1.2 calcium channels. J Biol Chem 286:8829–8838. https://doi.org/10.1074/jbc.M110.166520
57. Rougier JS, Albesa M, Syam N, Halet G, Abriel H, Viard P (2015) Ubiquitin-specific protease USP2-45 acts as a molecular switch to promote alpha2delta-1-induced downregulation of Cav1.2 channels. Pflugers Arch 467:1919–1929. https://doi.org/10.1007/s00424-014-1636-6
58. Ruan HB, Nie Y, Yang X (2013) Regulation of protein degradation by O-GlcNAcylation: crosstalk with ubiquitination. Mol Cell Proteomics 12:3489–3497. https://doi.org/10.1074/mcp.R113.029751
59. Seravalle G, Mancia G, Grassi G (2014) Role of the sympathetic nervous system in hypertension and hypertension-related cardiovascular disease. High blood press. Cardiovasc Prev. 21:89–105. https://doi.org/10.1007/s40292-014-0056-1
60. Sipido KR, Maes M, Van de Werf F (1997) Low efficiency of Ca2+ entry through the Na(+)-Ca2+ exchanger as trigger for Ca+ release from the sarcoplasmic reticulum. A comparison between L-type Ca2+ current and reverse-mode Na(+)-Ca2+ exchange. Circ Res 81:1034–1044. https://doi.org/10.1161/01.res.81.6.1034
61. Snow CM, Senior A, Gerace L (1987) Monoclonal antibodies identify a group of nuclear pore complex glycoproteins. J Cell Biol 104:1143–1156. https://doi.org/10.1083/jcb.104.5.1143
62. Trinidad JC, Barkan DT, Gulledge BF, Thalhammer A, Sali A, Schoepfer R, Burlingame AL (2012) Global identification and characterization of both O-GlcNAcylation and phosphorylation at the murine synapse. Mol Cell Proteomics 11:215–229. https://doi.org/10.1074/mcp.O112.018366
63. Wang DW, Kiyosue T, Shigematsu S, Arita M (1995) Abnormalities of K+ and Ca2 + currents in ventricular myocytes from rats with chronic diabetes. Am J Physiol 269:H1288–1296. https://doi.org/10.1152/ajpheart.1995.269.4.H1288
64. Watson LJ, Facundo HT, Ngoh GA, Ameen M, Brainard RE, Lemma KM, Long BW, Prabhu SD, Xuan YT, Jones SP (2010) O-linked beta-N-acetylglucosamine transferase is indispensable in the failing heart. Proc Natl Acad Sci U S A. 107:17797–17802. https://doi.org/10.1073/pnas.1001907107
65. Watson LJ, Long BW, DeMartino AM, Brittian KR, Readnower RD, Brainard RE, Cummins TD, Annamalai L, Hill BG, Jones SP (2014) Cardiomyocyte Ogt is essential for postnatal viability. Am J Physiol Heart Circ Physiol. 306:H142–153. https://doi.org/10.1152/ajpheart.00438.2013
66. Wu W, Zheng X, Wang J, Yang T, Dai W, Song S, Fang L, Wang Y, Gu J (2018) O-GlcNAcylation on Rab3A attenuates its effects on mitochondrial oxidative phosphorylation and metastasis in hepatocellular carcinoma. Cell Death Dis. 9:970. https://doi.org/10.1038/s41419-018-0961-7
67. Yang X, Qian K (2017) Protein O-GlcNAcylation: emerging mechanisms and functions. Nat Rev Mol Cell Biol 18:452–465. https://doi.org/10.1038/nrm.2017.22
68. Yokoe S, Asahi M, Takeda T, Otsu K, Taniguchi N, Miyoshi E, Suzuki K (2010) Inhibition of phospholamban phosphorylation by O-GlcNAcylation: implications for diabetic cardiomyopathy. Glycobiology 20:1217–1226. https://doi.org/10.1093/glycob/cwq071
69. Zhu WZ, El-Nachef D, Yang X, Ledee D, Olson AK (2019) O-GlcNAc transferase promotes compensated cardiac function and protein kinase A O-GlcNAcylation during early and established pathological hypertrophy from pressure overload. J Am Heart Assoc 8:e011260. https://doi.org/10.1161/jaha.118.011260